Computational Materials Science of Bionanomaterials: Structure, Mechanical Properties and Applications of Elastin and Collagen Proteins

28

Anna Tarakanova, Shu-Wei Chang, and Markus J. Buehler

Keywords

Materiomics • Elastin • Collagen • Hierarchical structure • Elasticity • Inverse temperature transition • Osteogenesis imperfecta (OI)

Introduction

Elastin and collagen can be thought of as complementary structural protein materials, having balanced roles in the function of the extracellular matrix. Elastin adds to the extensibility, while the more abundant collagen protein forms a robust framework within essential tissues. Here, we review the hierarchical structure of each protein, with an emphasis on mechanical signature and behavior. For elastin, we focus on the molecular and fiber level structure and mechanical properties that have been identified thus far, noting a missing fibril scale that has yet to be well-characterized. We go on to examine the molecular origins of two unique properties of elastin, namely, its ability to extend beyond multiple times its resting length and its unusual propensity to fold under higher temperatures, an effect known as the inverse temperature transition.

These authors Anna Tarakanova and Shu-Wei Chang contributed equally to this work

A. Tarakanova • S.-W. Chang
Laboratory for Atomistic and Molecular Mechanics (LAMM), Department of Civil and Environmental Engineering, Massachusetts Institute of Technology, Cambridge, MA, USA

M.J. Buehler (✉)
Laboratory for Atomistic and Molecular Mechanics (LAMM), Department of Civil and Environmental Engineering, Massachusetts Institute of Technology, Cambridge, MA, USA

Center for Computational Engineering, Massachusetts Institute of Technology, Cambridge, MA, USA
e-mail: mbuehler@mit.edu

B. Bhushan et al. (eds.), *Handbook of Nanomaterials Properties*,
DOI 10.1007/978-3-642-31107-9_14,

Both qualities render elastin an excellent template material for novel biomaterial applications and drug delivery devices, for example. In the section on collagen, we present recent finding of the molecular and fibril-scale signature of the protein, highlighting its multilevel hierarchy. We then outline a detailed case study of the disease *osoteogenesis imperfecta*, identifying molecular level origins and implications. We conclude with a section on applications and future directions in the study of these two important biomaterials.

Elastin

Tropoelastin: Precursor Molecule of Elastin

Elastin is an important extracellular matrix protein that is found in a wide range of tissues, including the skin, lung, heart, and arteries [1–4]. It is highly elastic, providing reversible deformability and recoil, with an ability to extend beyond several times its resting length and reversibly return to its original state, undergoing a lifetime of extension and compression cycles with minimal degradation. Elastic fibers are composed of a proteinaceous scaffold made up of several different proteins including fibrillins, fibulins, and glycoproteins, which acts as the base onto which elastin protein aggregates and assembles [5]. Elastin protein is made up of cross-linked soluble tropoelastin molecules, secreted from smooth muscle cells and fibroblasts, which are catalyzed by lysyl oxidase to make larger globules that assemble onto the scaffold (Fig. 28.1) [6].

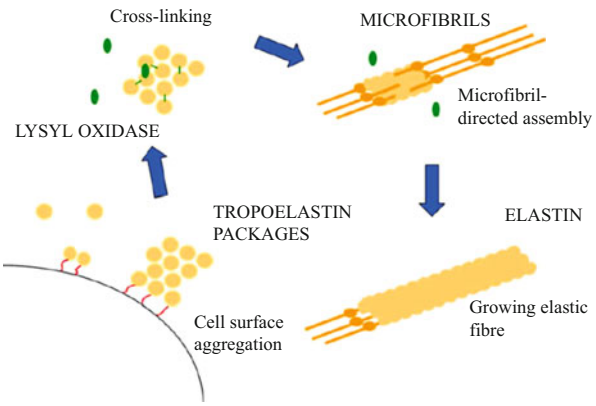

Fig. 28.1 Assembly mechanism of elastic fibers from tropoelastin molecules. Tropoelastin molecules assemble into larger globules, which are cross-linked with lysyl oxidase, forming larger clusters. Tropoelastin clusters assemble on microfibril scaffolds, forming a growing elastic fiber (Reprinted from Journal of Cellular Physiology, Kozel, B.A., et al., *Elastic fiber formation: A dynamic view of extracellular matrix assembly using timer reporters*, 2006. **207**(1): p. 87–96 with permission from Elsevier [6])

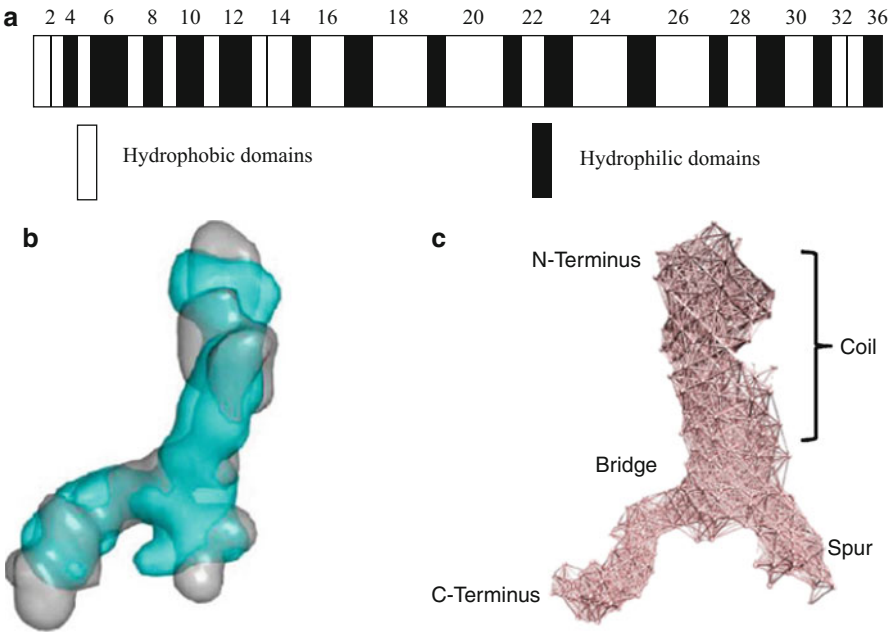

Fig. 28.2 (**a**) Structure of human tropoelastin gene with alternating hydrophobic and hydrophilic domains (Reprinted from Journal of Structural Biology, Wise, S.G., et al., *Specificity in the coacervation of tropoelastin*: *solvent exposed lysines*, 2005. **149**(3): p. 273–281 with permission from Elsevier [70]) (**b**) Averaged superimposed tropoelastin structures from small-angle x-ray (*blue*) and neutron (*gray*) scattering profiles (Reprinted with permission from [7]) (**c**) Full-length tropoelastin model (Adapted from [71])

Tropoelastin, elastin's soluble precursor molecule, is encoded by a single gene [5]. The most common isoform of tropoelastin is a 60 kDa molecule, consisting of 698 amino acids, composed of alternating hydrophilic and hydrophobic domains (Fig. 28.2a). Hydrophilic domains are involved in cross-linking, while the hydrophobic domains are believed to play a key part in the entropic elasticity of elastin. Hydrophobic domains are rich in glycine, alanine, valine, and proline residues, often occurring in repeating motifs of PGV, GVA, and GGV [5]. Hydrophilic domains are rich in lysines, which undergo irreversible cross-linking.

The globular structure of tropoelastin has recently been determined with small-angle x-ray and neutron scattering (Fig. 28.2b) [7]. Tropoelastin is an extended asymmetric molecule, with a 16-nm end-to-end distance and a width between 3 and 7.5 nm from its most narrow to its widest region. The N-terminus sits at the top of an extended cylinder of the molecular body. The cylinder contains an amorphous coiled region responsible for the elasticity of the molecule. Below the coil, the molecule splices into a spur region, thought to contain exons 20–24, which is

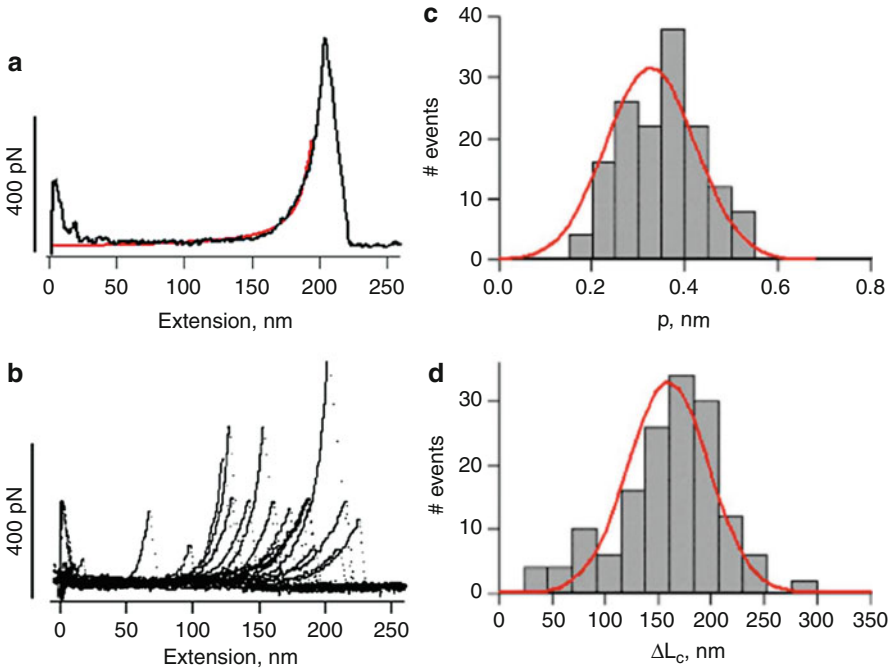

Fig. 28.3 (**a**) Sample single-molecule force-extension curve, with the *red line* representing worm-like chain model of a polymer with contour length of 211 nm and persistence length 0.38 nm. (**b**) 17 force-extension curves for stretching of tropoelastin molecules. (**c**) Frequency histogram for persistence length and (**d**) contour lengths, for 158 samples (Reprinted with permission from [7], Copyright (2011) National Academy of Sciences, U.S.A.)

connected to the cell-binding C-terminus foot region through a bridge, a highly exposed region, predisposed to cross-linking. The C-terminus region of tropoelastin has been found to be highly conserved across mammalian species (Fig. 28.2c) [7].

The mechanical signature of tropoelastin, that can reversibly extend to several times its resting length of 20 nm, with minimal energy loss, is a key factor in the overall superior mechanical properties of elastic fibers. Single tropoelastin molecules have been characterized by using atomic force microscopy, where molecules were stretched and relaxed sequentially (Fig. 28.3a, b). The force-extension patterns of tropoelastin molecules fit well to a worm-like chain model, with a persistence length of 0.36 calculated for an average contour length of 166 nm, suggesting high molecular elasticity (Fig. 28.3c, d). The Young's modulus was calculated to be approximately 3 kPa [7].

Elastic Fibers: Structure and Mechanical Properties

Elastin fibers are the largest structural unit composing tissues. Water-swollen elastic fibers are approximately 1–8 μm in diameter (Fig. 28.4a) [5, 8]. Elastic

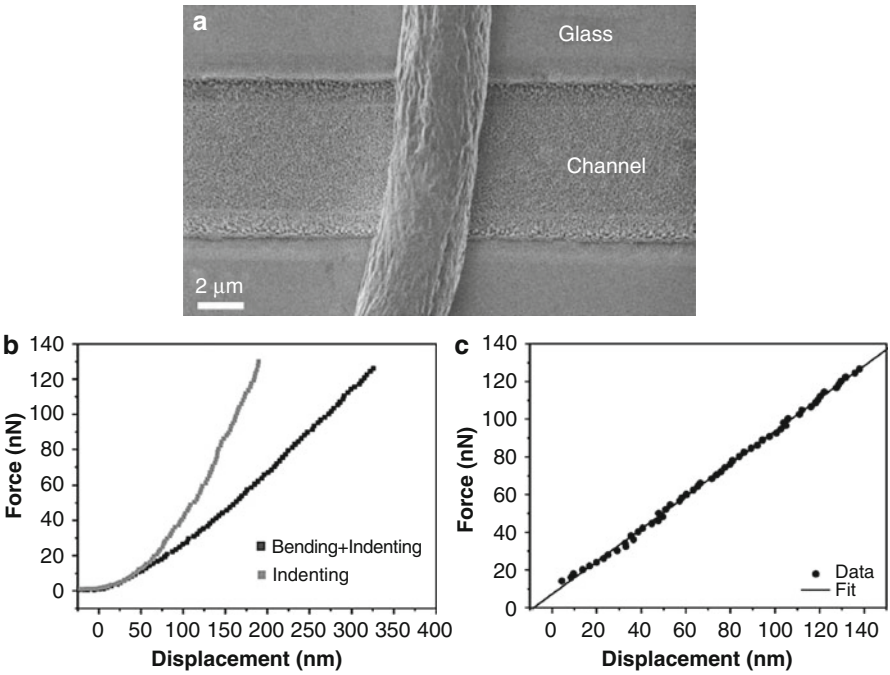

Fig. 28.4 (**a**) SEM image of an elastic fiber in a micro-channel of a glass substrate. (**b**) Force-displacement curve for indenting elastic fiber on the glass substrate (*black*) and bending the fiber in the middle, with indentation. (**c**) Force-displacement curve representing bending only (Reprinted from Biomaterials, Koenders, M.M.J.F., et al., *Microscale mechanical properties of single elastic fibers*: *The role of fibrillin-microfibrils*, 2009. **30**(13): p. 2425–2432 with permission from Elsevier [11])

fibers have been observed to be twisted and straight, arranged as interwoven networks or as flattened sheets, depending on tissue type [8]. Elastin networks can generally be found in connective tissue, while dense tissue such as the aorta is composed of flattened elastin sheets, or elastic laminae [8]. Elastin fibers have been extensively studied, with various studies identifying a supramolecular fibrillar organization within fibers. Scanning electron microscope (SEM) studies have found that elastin fibers from bovine fetal and adult samples are composed of fibrils 100–130 nm in diameter, where thickening occurs during maturation [9, 10]. Thicker fibrils in adult tissue may be due to aggregation of smaller filaments onto the fibrils. Further down the length-scale hierarchy, filaments of about 1 nm up to 8 nm have been observed within fibrils, arranged parallel to the main fiber axis, and sometimes exhibiting helical or twisted configuration with some cross-bridging [9]. Variable sizes were observed depending on whether a stretched or relaxed configuration was considered, with smaller sizes corresponding to stretched configurations [9]. Stretched filaments also showed better alignment than relaxed filaments.

Elastic tissue and fiber mechanics have been well studied, but substructure filaments and fibrils are yet to be characterized as a result of the difficulty in isolating these substructures, due to high levels of cross-linking and their propensity to aggregate. Macro-mechanical testing has been used for years to study elastin-rich tissue samples. Studies from dog, sheep, and pig aorta determined the Young's modulus of the elastic fiber-rich tissue to be in the range of 0.1–0.8 MPa [11–13]. The Young's modulus of single elastin fibers was first determined from bovine ligamentum nuchae samples to be in the range of 0.4–1.2 MPa, by using a microtesting apparatus attached to a polarizing microscope [14]. A later study comparing fibrillin-rich and fibrillin-free elastin fibers revealed a similar Young's modulus of 0.90 and 0.79 MPa, respectively, though the statistical difference was not significant, signifying that scaffolding microfibrils do not significantly influence the mechanical properties of single elastic fibers [11]. Here, a tip-less Atomic Force Microscope (AFM) cantilever was used to bend freely suspended fibers on a microchanneled substrate. A displacement from bending and local indentation was induced by exerting a force at the middle point of the channel, and the modulus was determined by subtracting the force-displacement curve derived from local indentation only (Fig. 28.4b, c). A linear force-displacement curve was found for fibers with and without microfibrils [11].

Entropic Origins of Elastin's Elasticity

Three prevalent hypotheses have guided the understanding of elastin's elasticity for the past half century: the classical theory of rubber elasticity, the hydrophobic effect, and librational entropic mechanisms [1]. Initially, elastin's superb elasticity was attributed to the classical theory of rubber elasticity, first proposed by Hoeve and Flory [15]. This model assumed that elastin was a single-phase system with randomly configured polymeric chains which assume a highest entropy at lowest end-to-end extension, such that any displacement from this highest entropy state is responsible for the elastic restoring force [15, 16]. This model failed to explain certain elements key to elastin's performance, such as the requirement for water [17].

Computationally intensive molecular dynamics (MD) simulation studies began to shift away from the rubber elasticity viewpoint, first with Urry's proposal of an alternative librational elasticity mechanism, suggesting that the elastic restoring force originates from a reduction in available configuration space upon extension as the peptide segments are stretched [18]. Chang and Urry first conducted molecular dynamics studies on the elastomeric polypentapeptide $(VPGVG)_7$ [19], finding that the total energy was lower by 15 kcal/mol for the relaxed state than for the extended state, which was primarily attributed to the difference in the van der Waals term, and could be explained by the greatly reduced side chain interactions in the extended state. They found that the number of accessible amplitudes of torsional libration in the linker residues bridging different segments was reduced as the structure was extended, suggesting a librational entropic mechanism.

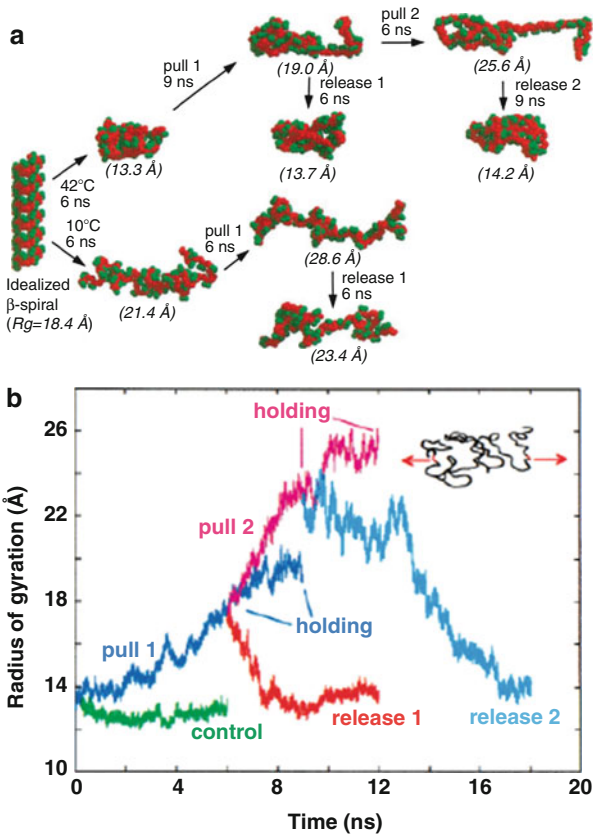

Fig. 28.5 (**a**) Conformational structures during pull and release cycles, at 10 °C and 42 °C, starting from an initial β-spiral configuration, with radius of gyration in parentheses. (**b**) Radius of gyration for the system at 42 °C for two pull and release cycles (Reprinted with permission from Li, B. and V. Daggett, *Hydrophobic Hydration Is an Important Source of Elasticity of Elastin*. Journal of the American Chemical Society, 2001. **123**: p. 11991–11998. Copyright 2001 American Chemical Society [22])

The second alternative idea was suggested by Gosline [20] proposing that the hydrophobic effect guided protein-water interactions, accounting for elastin's elasticity. Wasserman studied elastin-like polypeptide $(VPGVG)_{18}$, concluding that hydrophobic interactions in the initial regimes of elastic stretching contribute to elastin entropy at low extensions, but that librational mechanisms are more significant at longer extensions [21]. Further studies have since yielded further evidence against the original classic rubber elasticity proposal. Li et al. carried out MD simulations in explicit water for the same elastin-like polypeptide $(VPGVG)_{18}$ but with longer trajectory lengths, at two different temperatures, 10 °C and 42 °C (Fig. 28.5a) [22]. They found that the extended state of the peptide at both temperatures had a large solvent-accessible surface area and a low number of hydrophobic contacts in the extended state. Upon release, the surface area and the number of hydration waters decreased, while the number of interchain contacts increased (Fig. 28.5b). Their finding suggested that the orientational entropy of the water, rather than the number of main-chain polar hydration waters as well as the release of hydration waters, is responsible for the

elasticity of the system. Altogether, these studies point to a dual entropic effect to describe elastin's elasticity: a combination of the hydrophobic entropic effect and a librational entropic effect [19, 21–26].

Inverse Temperature Transition of Elastin

Another fundamental property of elastin and elastin-like peptides (ELPs) is its propensity to fold to a more stable configuration with higher temperatures, an effect termed an inverse temperature transition (ITT) [1]. Several studies have observed filament formation in aqueous solution upon increasing temperature in elastin fragments and in ELPs [27, 28]. From these observations, elastin and ELPs have been suggested as effective candidates for "biomolecular machines," converting chemical, electrical, and particularly thermal signals into other forms of energy, such as reversible contraction [29].

Several computational studies have looked at elastin's ITT. Li et al. studied the ITT using the elastin-like polypeptide, $(VPGVG)_{18}$, considering dynamics at seven temperatures ranging from 7 °C to 42 °C (Fig. 28.6a) [30]. At higher temperatures solvent-accessible surface area of the polypeptide and the number of hydration

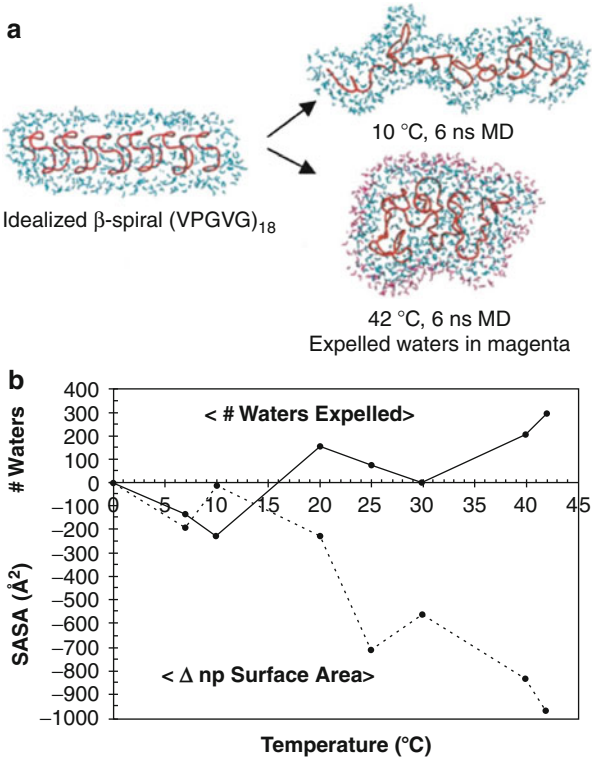

Fig. 28.6 (**a**) Conformational change resulting from an inverse temperature transition. 6 ns trajectories are recorded for the same starting structure at temperatures of 10 °C and 42 °C. (**b**) The number of expelled waters increases, while the surface area exposed to hydration decreases as temperature increases beyond the transition temperature (Reprinted from the Journal of Molecular Biology, Li, B., D.O. Alonso, and V. Daggett, *The molecular basis for the inverse temperature transition of elastin*, 2001. **305**(3): p. 581–92 with permission from Elsevier [30])

waters decreased, while intra-chain contacts increased, as had been observed in the released state of the polypeptide following extension in elasticity studies (Fig. 28.6b).

Marx et al. considered the elastin-like octapeptide GVG(VPGVG), finding a two-state system near the transition temperature [31]. They showed that at low temperatures, strong peptide/water interactions stabilize open conformations, while an increase in temperature above transition decreases the stability of the extended state but has less effect on the folded conformation. The folded conformation is stabilized by intermolecular hydrogen bonds as well as by an entropic increase in backbone fluctuation, though eventually the highly dynamic system unfolds at still higher temperatures [31].

Based on elastin's unique inverse temperature transition, several studies have explored the effect of directly manipulating elastin-like polypeptides to probe their capacity to act as molecular switch systems [1]. MD simulations of wild-type chymotrypsin inhibitor 2 (CI2) and variants containing elastin-like turns were performed at 10 °C and 40 °C, with a result yielding wild-type CI2 that was more stable at 10 °C, while both of the variant forms were more stable at 40 °C [23]. This suggests that elastin-like peptides could be used to stabilize target proteins, for example. Arkin and Bilsel [32, 33] considered the effects of single-residue substitutions in the elastin-like sequence VPGXG as well as the polypeptide length as a governing factor influencing the transition temperature. They found that the ITT was highly dependent on residue specificity and polypeptide length, identifying switchable parameters for tuning materials. These studies confirm the validity and applicability of the unique quality of elastin to undergo an inverse temperature transition, opening an important new direction in material design to create controllably mutable elastin-based materials.

Collagen

Structure of Collagen Molecules

Collagen is the most abundant protein in the vertebrate and, like elastin, the basic component of connective tissues. It provides mechanical strength and biological functions for connective tissues [34–37]. A collagen molecule consists of three chains stacked alongside forming a triple helix structure, as shown in Fig. 28.7. Each chain of a collagen molecule consists of amino acids and has a characteristic repeating sequence of $(\text{Gly-X-Y})_n$. The spheres in Fig. 28.7 represent the alpha-carbon atoms of Gly residues, which are mostly located within the center of a collagen molecule. The triple helix structure is stabilized by hydrogen bonds between each chain. About 28 types of collagen have been identified while type I collagen, which is found in tendon, skin, teeth, cornea, and bone, is the most abundant collagen in the human body. A type I collagen molecule has a length of about 300 nm with a radius of approximately 1.6 nm.

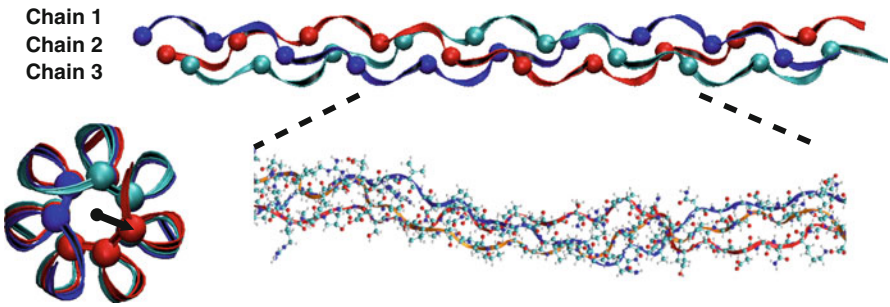

Fig. 28.7 Molecular structure of a collagen molecule, which consists of three chains forming a triple helix structure. Each chain is plotted with one color, and the spheres represent the alpha-carbon atoms of glycine residues. The collagen molecule has a characteristic sequence of $(\text{Gly-X-Y})_n$. The triple helix structure is stabilized by interchain hydrogen bonds

The collagen molecule is a heterogeneous structure along its twisting axis due to the variation of amino acid sequence. The variation of sequence is crucial for varied biological functions along each segment of the collagen molecule. A collagen molecule has a varying unit height of ~0.853 nm for imino-rich regions and ~0.865 nm for amino-rich regions [38]. Triple helix builders, such as GENCOLLAGEN [39] and THeBuScr [40], have been developed recently to create idealized atomic coordinates by using sequence information of collagen. Variation of sequence also affects the thermal stability of local conformation of a collagen molecule. Persikov et al. have developed a thermal stability calculator for collagen based on experimental measurements [41]. Figure 28.8 shows examples of relative thermal stability profiles for full-length type I and type II collagen molecules. It identifies a nonuniform distribution of thermal stability along the entire length of the molecule. The highest thermal stability are found at the N- and C-terminals, which impacts the mechanical and biological properties. For example, the two regions with low stability in the type I collagen molecule (indicated by arrows in the figure) are identified to be the cross-linking sites.

Hierarchical Structure of Collagen-Based Tissues

Collagen molecules are the basic building blocks of connective tissue, having a hierarchical structure as illustrated in Fig. 28.9. Collagen molecules, produced by cells, are stacked together in a characteristic *D*-period to form collagen fibrils which have diameters of ~100 nm. Collagen fibrils are the basic components of collagen fiber which forms connective tissues. The orientation of collagen fibrils varies in different connective tissues to provide particular mechanical and biological functions. In tendon and bone, collagen fibrils align mostly parallel

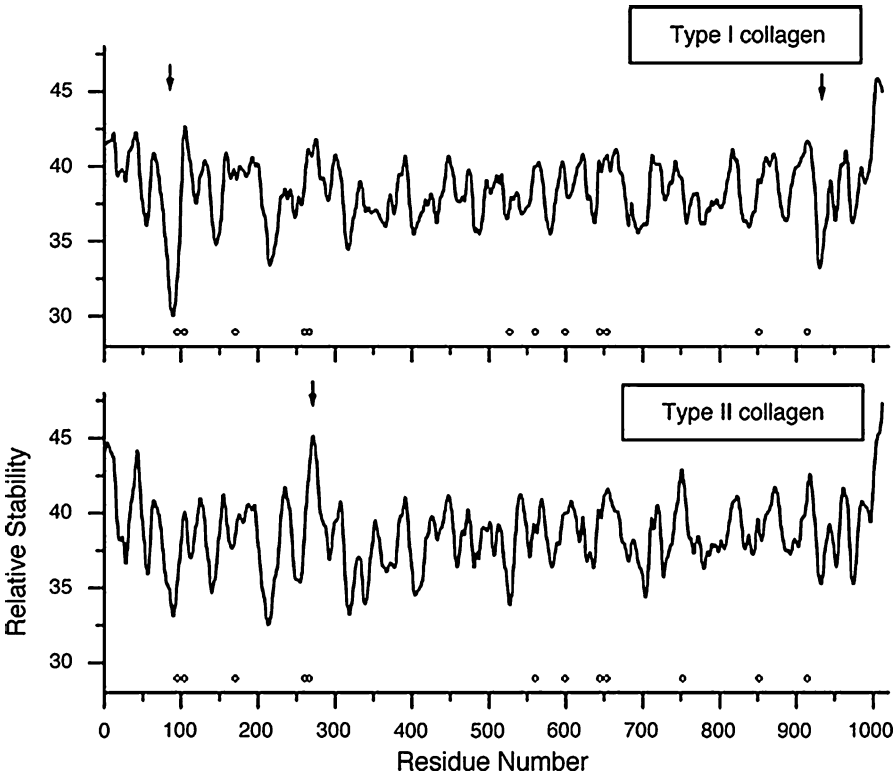

Fig. 28.8 Calculated relative thermal stability of type I and type II collagen along the twisting axis. Collagen molecule is a heterogeneous material along its length. The variation of sequence impacts its material and biological properties (Reprinted from [41] with permission)

to each other to provide mechanical strength in the axial direction of the tissue. In the cornea, collagen fibrils align radially to form a membrane structure. Alignment also varies across animals species to provide specific biomechanical properties [42].

Structure of the Collagen Fibril

Recently, the in situ structure of the full-length type I collagen fibril (Protein Data Bank identification code 3HR2) has been revealed [43], as shown in Fig. 28.10. The collagen fibril has a triclinic unit cell with dimensions $a \sim 40.0$ Å, $b \sim 27.0$ Å, $c \sim 678$ Å, $\alpha \approx 89.2^{o}$, $\beta \approx 94.6^{o}$, $\gamma \approx 105.6^{o}$. A fibril has a gap region with a length of 0.54 D and an overlap region with a length of 0.46 D (Fig. 28.10). Here D ($\sim$67 nm) denotes the length of the D-period of collagen fibril. Overlap and gap regions have different biological properties. The cell interaction domain of

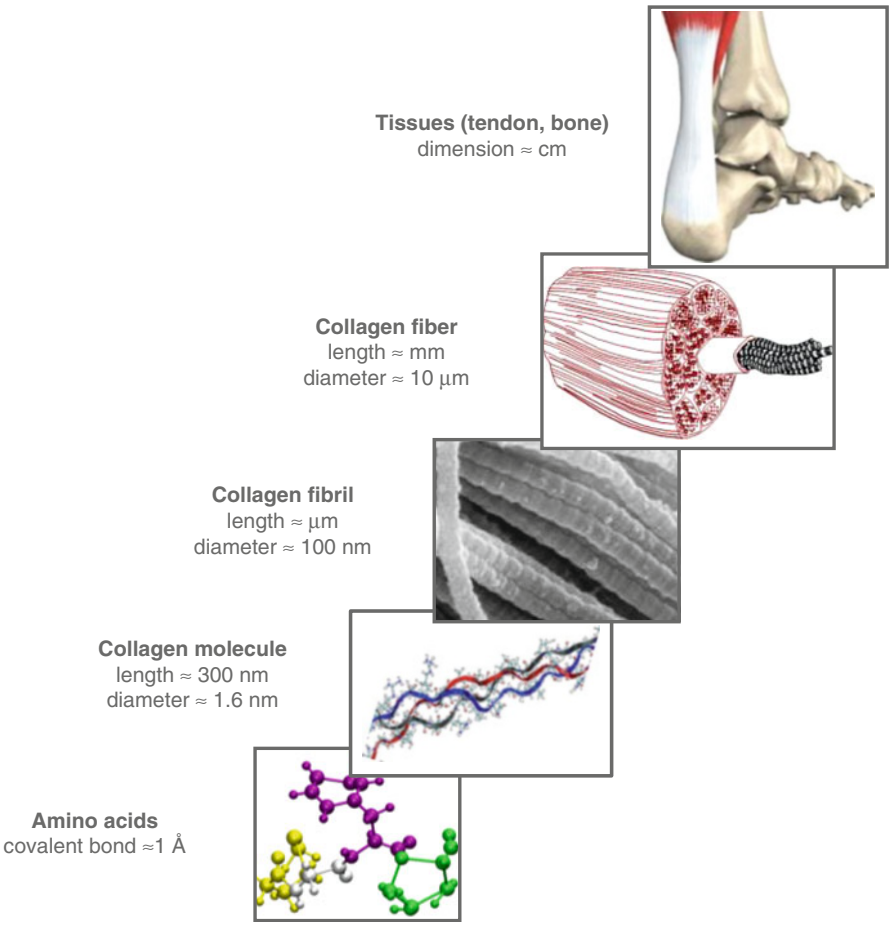

Fig. 28.9 Hierarchical structure of collagenous tissues, from the atomistic level to the tissue level. Collagen molecules pack to form collagen fibrils with diameter of ~100 nm. Connective tissues such as tendon and bone consist of collagen fibers, formed by bundles of collagen fibrils (Reprinted with permission from Gautieri, A., et al., *Hierarchical structure and nanomechanics of collagen microfibrils from the atomistic scale up*. Nano Letters, 2011. **11**(2): p. 757–66. Copyright 2011 American Chemical Society)

collagen has been linked to the overlap region, while tissue mineralization occurs in the gap region [44]. The length of the *D*-period of the collagen fibril has slightly different values for different tissues. The *D*-period is about 67 nm for tendon and bone which contains primarily type I collagen. Skin, which contains about 15 % type III and 85 % type I collagen, has been shown to have a slightly shorter *D*-period of ~65 nm [45–47].

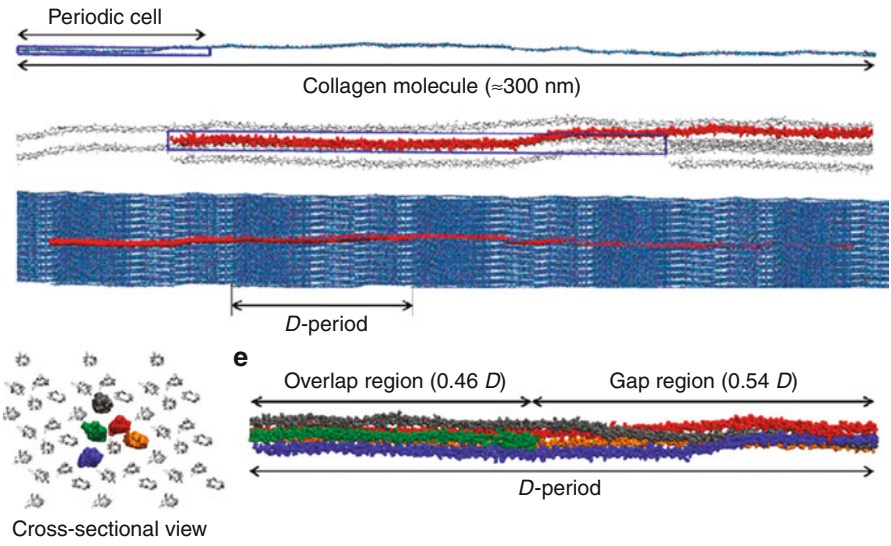

Fig. 28.10 A periodic cell of a collagen fibril model. Collagen molecules packing in a specific arrangement form a *D*-period of ~67 nm, which contains an overlap region and a gap region. The in situ structure of full-length type I collagen fibril is revealed by Orgel et al. [72]. The figure shows a full atomistic model of human collagen fibril, which is reprinted with permission from Gautieri, A., et al., *Hierarchical structure and nanomechanics of collagen microfibrils from the atomistic scale up*. Nano Letters, 2011. **11**(2): p. 757–66. Copyright 2011 American Chemical Society

Collagen Mechanics

Mechanical Properties of a Single Collagen Molecule

A typical force-displacement curve of a single collagen molecule is shown in Fig. 28.11. For mechanical forces below 14 pN, a collagen molecule is flexible and behaves in a worm-like chain behavior [48–50]. This is the entropic elasticity regime of a collagen molecule, where the molecule exhibits large strain which may play a role in cell signaling. Collagen molecules have persistence lengths in the range of 10–15 nm, depending on collagen type. Mechanical tests using optical tweezers have shown a persistence length of 14.5 ± 0.73 nm for type I collagen [51] and a persistence length of 11.2 ± 8.4 nm for type II collagen [49]. Atomistic simulations have predicted a similar range of the persistence length of collagen [50, 52]. Although the worm-like chain model can describe the force-displacement curve of a collagen molecule quite well overall, the collagen molecule is known to feature nonuniform deformation throughout its length due to the variations of sequence.

The mechanical properties of a collagen molecule vary along its twisting axis, and the local conformations are known to change and have different biological functions [44]. There exist micro-unfolding regions in a collagen

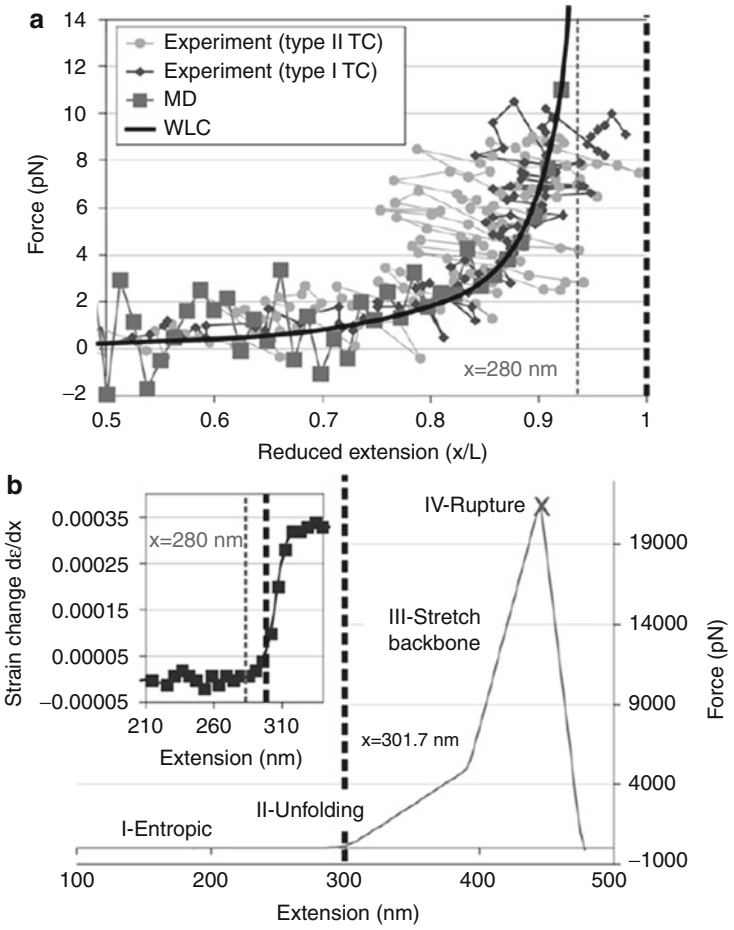

Fig. 28.11 Mechanical response of a single collagen molecule. When exposed to a mechanical force below ~14 pN, the collagen molecule behaves like a flexible worm-like chain with a persistence length of ~10–15 nm. This is the entropic elasticity regime of a collagen molecule. When mechanical force is larger than ~14 pN, there are three regimes in a force-displacement curve of a collagen molecule. The collagen molecule is uncurling first followed by stretching backbone covalent bonds and then rupture (Reprinted from Biophysical Journal, Buehler, M.J. and S.Y. Wong, *Entropic Elasticity Controls Nanomechanics of Single Tropocollagen Molecules*., 2007. **93**(1): p. 37–43., Copyright 2007, with permission from Elsevier [50])

molecule [52–54]. Micro-unfolding regions are thought to be important for biological functions such as collagen degradation. When a collagen molecule is stretched in the entropic elasticity regime, the mechanical force induces larger deformations in the micro-unfolding regions (as they are softer), while only inducing small deformation for regions that have higher thermal stability [53]. The mechanical response of a collagen molecule in the entropic elasticity regime is likely relevant

for its biological functions. For example, recent studies have shown that low mechanical force in the order of pN is sufficient to alter the collagen degradation rate greatly [55–57].

Once a collagen molecule is pulled out of the entropic elasticity regime, there are three other regimes [50]. Firstly, the collagen molecule undergoes uncurling through its entire length. In this regime, the collagen molecule is likely to feature a more uniform strain distribution since micro-unfolding regions have already been stretched [53]. Earlier experimental and computational studies revealed that the Young's modulus of a collagen molecule is in the range of 3–9 GPa [51, 53, 58–62]. Further stretching a collagen molecule will induce stretching of the backbone of each chain, resulting in a markedly stiffer response. In the last regime, a collagen molecule is ruptured if it is deformed beyond its strength.

Mechanical Properties of Collagen Fibrils

The mechanical response of collagen fibrils is distinct from collagen molecules. The mechanical features of a collagen microfibril obtained from a molecular model are shown in Fig. 28.12. For a hydrated collagen fibril, two regimes have been

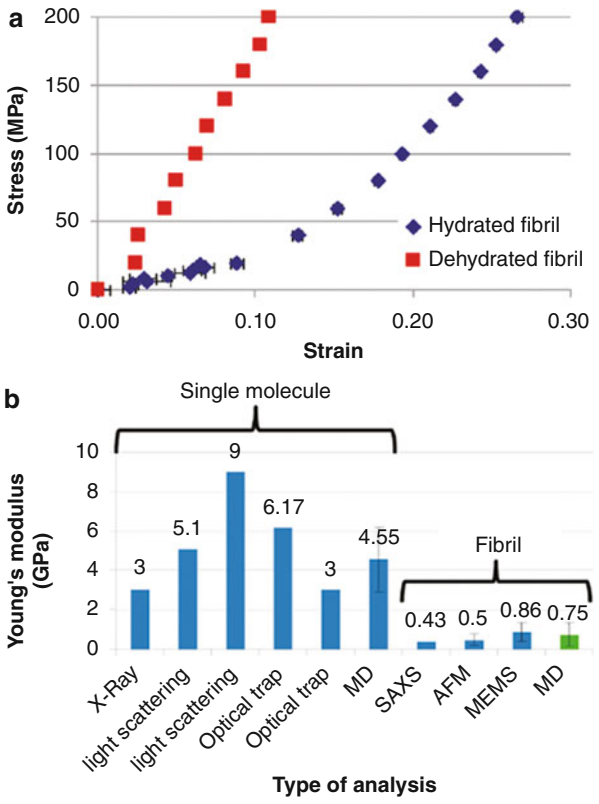

Fig. 28.12 (**a**) Mechanical response of a hydrated and dehydrated collagen fibril. A dehydrated collagen fibril has a linear stress–strain curve, while a hydrated collagen fibril has two regimes. In the first regime of a hydrated collagen, the collagen fibril exhibits nonlinear relations, while in the second regime, the collagen fibril, it is stiffer and has a linear stress–strain relation. (**b**) Young's modulus of single collagen molecules and collagen fibrils obtained from various experimental and computational studies (Reprinted with permission from Gautieri, A., et al., *Hierarchical structure and nanomechanics of collagen microfibrils from the atomistic scale up*. Nano Letters, 2011. **11**(2): p. 757–66. Copyright 2011 American Chemical Society)

identified in the stress–strain curve. In the first regime (strain below ~10 % and stress below ~50 MPa), the collagen fibril has a nonlinear and softer mechanical response. The end-to-end distance of a collagen molecule within the fibril is increased in this region, which suggests that the micro-unfolding domains are stretched. The extensibility of a collagen fibril in this regime is important for cell-matrix interactions and for many biological functions. Once the stress in a collagen fibril reaches ~50 MPa, the end-to-end distance of a collagen molecule reaches its contour length, indicating that it has been straightened. Atomistic simulations have revealed that the straightening of a collagen molecule happens primary in the gap region [62]. Beyond this point, the stress–strain curve of a collagen fibril enters the second regime which has a linear behavior. Because the collagen molecule has been straightened, the collagen fibril becomes stiffer in this regime (Fig. 28.12).

A hydrated collagen fibril has a Young's modulus of ~300 MPa at small strain and a modulus of ~1.2 GPa at large strain [62], while a dehydrated fibril has a larger modulus of ~2 GPa independent of the applied stress. Figure 28.12b shows values of the Young's modulus of collagen molecules and fibrils from various experimental studies and molecular simulations. A collagen fibril has been found to have a smaller modulus ~0.4–0.9 GPa compared with a single collagen molecule, which features a modulus ~3–9 GPa. These data suggest a strong scale and environment dependence of collagen properties.

Mutations and Diseases in Collagen-Based Tissues

Single-residue mutations in collagen molecules have been identified and associated with various diseases. For example, *osteogenesis imperfecta* (OI), which is known as brittle bone disease, is a rare genetic disorder of collagenous tissues. The OI mutation is caused primarily by a replacement of the Gly residue in the repeating $(Gly\text{-}X\text{-}Y)_n$ triplets. In brittle bone disease, mutations at a single-molecule level alter the material properties of collagenous tissue at macroscale. As of now, several mutation locations and types along the entire collagen molecule have been identified and classified into severe, moderate, and mild disease conditions, as shown in Fig. 28.13 [63].

Although it remains unclear how a mutation of a collagen molecule could lead to a change in the material property of collagenous tissues, recent studies have revealed that mutations in the molecule cause changes in its structure and mechanical properties [64] at the molecular level. The OI mutations are found to disrupt the triple helix structure of the collagen molecule in the vicinity of the mutation. The unfolding of the triple helix structure at the mutation site results from the disruption of interchain hydrogen bonds. The severity of structure disruption is found to depend on mutation phenotype (Fig. 28.14).

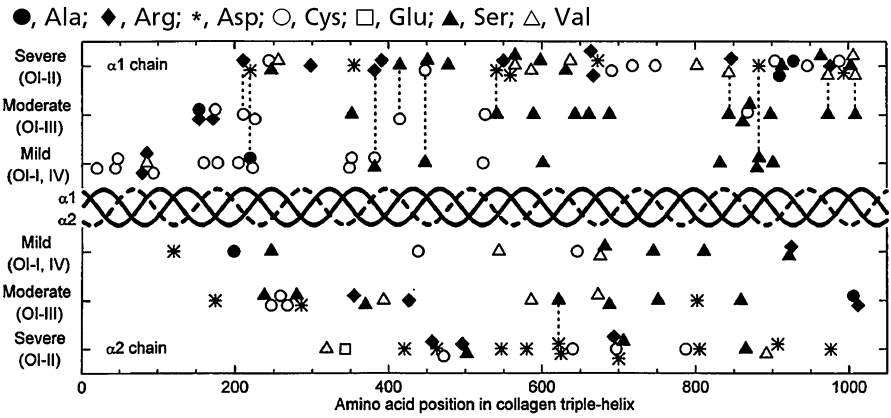

Fig. 28.13 Mutations throughout the entire type I collagen molecule which have be identified to cause severe, moderate, and mild OI (Reprinted from [63], Copyright (2000) National Academy of Sciences, U.S.A.)

There is a strong correlation with the severity of the phenotype and the interchain distance at energy minimum. Experimental studies have shown that the severity of the phenotype can be correlated to the decrease of melting temperature of the collagen molecule, indicating that the reduction of thermal stability caused by the OI mutation is a critical aspect to understand brittle bone disease. The OI mutations have also been shown to cause reductions in the Young's modulus of collagen molecules [65].

The change in the chemical composition of collagen molecules not only affects the properties at the single collagen molecule level (Fig. 28.14) but also alters the properties of collagen tissues. The *osteogenesis imperfecta* mouse model, *oim*, is also caused by mutations in the collagen molecule. In the case of *oim* mutations, the alpha-2 chain of the collagen molecule is replaced by an alpha-1 chain, resulting in a homotrimer molecule. Experimental studies of *oim* mice bone and tendon have shown reduced mechanical strength compared to normal mice. As shown in Fig. 28.15a, material properties of 1-year-old mice have been measured to examine the severity of phenotype [66]. The *oim*/*oim* mice are found to have significant reductions of their failure torque and torsional stiffness compared with normal bone. On the other hand, experimental studies of mouse tail tendon have shown that the *oim* mouse fiber from tail tendon has a higher denaturation temperature compared with normal mice (Fig. 28.15b) [67], indicating that the mutation alters the packing of collagen molecules. These data suggests that the material properties of collagen molecules, which are controlled by their chemical compositions, have a great impact on larger-scale structure and mechanical properties of collagen-based tissues.

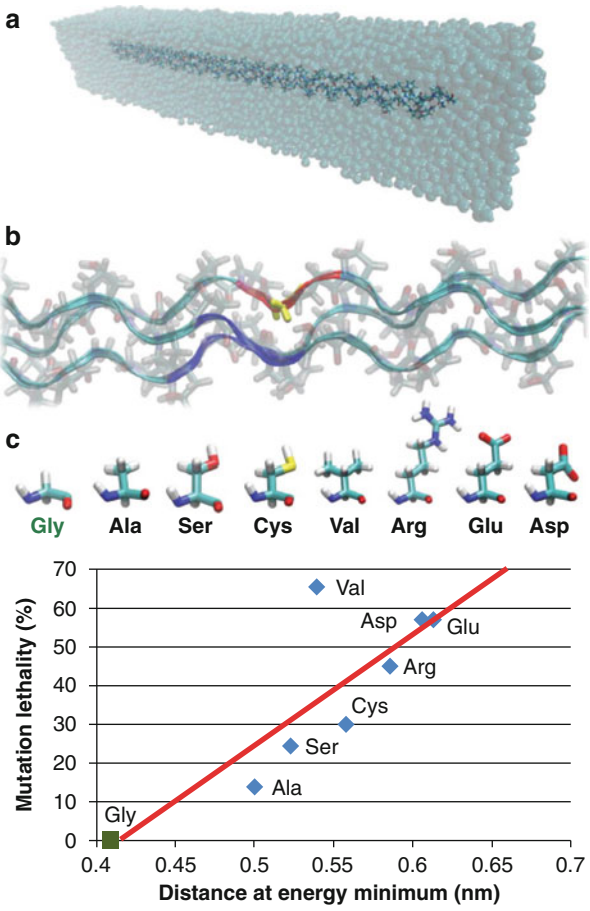

Fig. 28.14 Atomistic simulations on the structural alterations causing by OI mutations. (*Panel a*) shows the atomistic simulation model. (*Panel b*) shows the selected mutation site. (*Panel c*) shows the mutation types which have been studied. The figure on the *right* shows the correlation between OI phenotype and collagen unfolding (Reprinted from [64])

Conclusions and Applications

The structure, superb mechanical properties, and unique biological properties of elastin and collagen proteins make them distinctive biomaterials. Applications of elastin-based and collagen-based biomaterials are numerous. Elastin can be used to create tunable electrospun elastin fiber scaffolds for large-scale tissue repair; elastin hydrogels are ideal for creating biodegradable matrices for drug delivery; elastin-based synthetic fibers can be used as prototypes for tissue engineering and artificial arteries [4]. Elastin-based tissue replacements are in high demand as elastin's low thrombogenicity, capacity for favorable cell interactions, and blood compatibility make it an ideal candidate for dermal and vascular substitutes for tissue regeneration [68]. Artificial collagen-based materials hold great opportunity in many biological and pathological applications [69]. For example, collagen sponges have been used to improve in vitro growth of many types of tissue. A molecular level

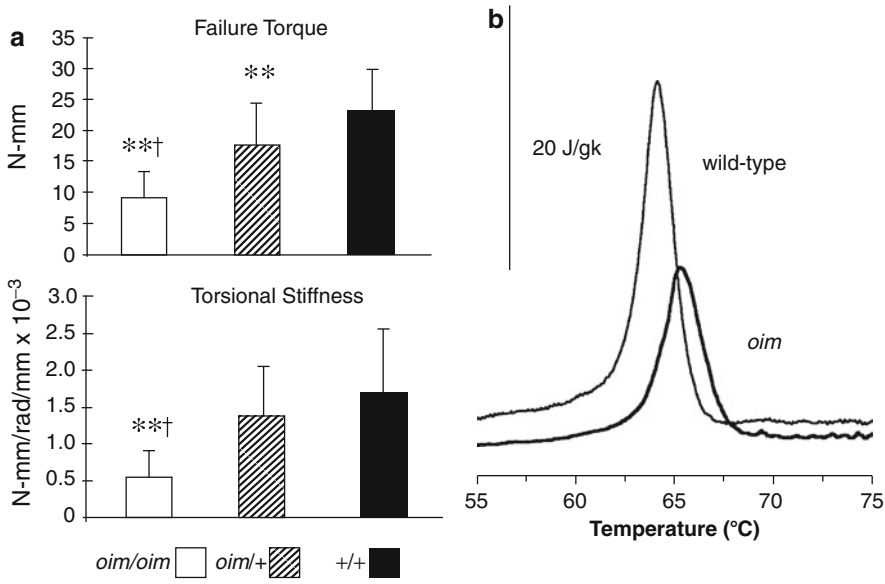

Fig. 28.15 (**a**) Failure torque and torsional stiffness of bone from *oim* and normal mice (Reprinted from [66] with permission). (**b**) Thermograms of tail tendon of wild-type and *oim* mice in water. The *oim* mice fibers have higher denaturation temperature, indicating that the mutation alters the packing of collagen molecules (Reprinted from *J. Mol. Biol.*, Miles, C.A., et al., The role of alpha2 chain in the stabilization of the collagen type I heterotrimer: a study of the type I homotrimer in oim mouse tissues, 2002. **321**: p. 797–805., Copyright 2002, with permission from Elsevier [67])

understanding, with the help of computational studies of these outstanding functionalities, holds great promise for tissue engineering applications and development of new, nature-inspired biomaterials, even surpassing material properties of elastin and collagen.

References

1. Tarakanova A, Buehler MJ (2013) Molecular modeling of protein materials: case study of elastin. Modelling and Simulation in Materials Science and Engineering 21(6):063001
2. Rosenbloom J et al (1995) Structure of the elastin gene. Ciba Foundation Symposium 192: The Molecular Biology and Pathology of Elastic Tissues 59–80
3. Debelle L, Alix AJP (1999) The structures of elastins and their function. Biochimie 81(10):981–994
4. Wise SG, Mithieux SM, Weiss AS (2009) Engineered tropoelastin and elastin-based biomaterials. Adv Protein Chem Struct Biol 78:1–24
5. Muiznieks LD, Weiss AS, Keeley FW (2010) Structural disorder and dynamics of elastin. Biochem Cell Biol Biochim Biol Cell 88(2):239–250
6. Kozel BA et al (2006) Elastic fiber formation: a dynamic view of extracellular matrix assembly using timer reporters. J Cell Physiol 207(1):87–96

7. Baldock C et al (2011) Shape of tropoelastin, the highly extensible protein that controls human tissue elasticity. Proc Natl Acad Sci USA 108(11):4322–4327
8. Ushiki T (2002) Collagen fibers, reticular fibers and elastic fibers. A comprehensive understanding from a morphological viewpoint. Arch Histol Cytol 65(2):109–126
9. Pepe A, Bochiechio B, Tamburro AM (2007) Supramolecular organization of elastin and elastin-related nanostructured biopolymers. Nanomedicine 2(2):203–218
10. Kewley MA, Steven FS, Williams G (1977) Presence of fine elastin fibrils within elastin fiber observed by scanning electron-microscopy. J Anat 123:129–134
11. Koenders MMJF et al (2009) Microscale mechanical properties of single elastic fibers: the role of fibrillin-microfibrils. Biomaterials 30(13):2425–2432
12. Lillie MA, David GJ, Gosline JM (1998) Mechanical role of elastin-associated microfibrils in pig aortic elastic tissue. Connect Tissue Res 37(1–2):121–141
13. Sherebrin MH (1983) Mechanical anisotropy of purified elastin from the thoracic aorta of dog and sheep. Can J Phys Pharmacol 61(6):539–545
14. Aaron BB, Gosline JM (1981) Elastin as a random-network elastomer – a mechanical and optical analysis of single elastin fibers. Biopolymers 20(6):1247–1260
15. Hoeve CA, Flory PJ (1974) The elastic properties of elastin. Biopolymers 13(4):677–686
16. Hoeve CA, Flory PJ (1958) The elastic properties of elastin. J Am Chem Soc 80:6523–6526
17. Partridge SM (1962) Elastin. Adv Protein Chem 17:227–302
18. Urry DW, Venkatachalam CM (1983) A librational entropy mechanism for elastomers with repeating peptide sequences in helical array. Int J Quantum Chem 10:81–93
19. Chang DK, Urry DW (1988) Molecular dynamics calculations on relaxed and extended states of the polypentapei'tide of elastin. Chem Phys Lett 147(4):395–400
20. Gosline JM, Yew FF, Weisfogh T (1975) Reversible structural-changes in a hydrophobic protein, elastin, as indicated by fluorescence probe analysis. Biopolymers 14(9):1811–1826
21. Wasserman ZR, Salemme FR (1990) A molecular dynamics investigation of the elastomeric restoring force in elastin. Biopolymers 29:1613–1631
22. Li B, Daggett V (2001) Hydrophobic hydration is an important source of elasticity of elastin. J Am Chem Soc 123:11991–11998
23. Li B, Alonso DOV, Daggett V (2002) Stabilization of globular proteins via introduction of temperature-activated elastin-based switches. Structure 10(7):989–998
24. Huang JX et al (2012) On the inverse temperature transition and development of an entropic elastomeric force of the elastin mimetic peptide [LGGVG](3,7). J Chem Phys 136(8):085101
25. Rauscher S et al (2006) Proline and Glycine control protein self-organization into elastomeric or amyloid fibrils. Structure 14(11):1667–1676
26. Ma X et al (2012) Thermal hysteresis in the backbone and side-chain dynamics of the elastin mimetic peptide [VPGVG](3) by H-2 NMR. J Phys Chem B 116(1):555–564
27. Cox BA, Starcher BC, Urry DW (1973) Coacervation of α-elastin results in fiber formation. Biochim Biophys Acta 317:209–213
28. Urry DW (1988) Entropic elastic processes in protein mechanisms.1. elastic structure due to an inverse temperature transition and elasticity due to internal chain dynamics. J Protein Chem 7(1):1–34
29. Urry DW (1995) Elastic biomolecular machines. Sci Am 272(1):64–69
30. Li B, Alonso DO, Daggett V (2001) The molecular basis for the inverse temperature transition of elastin. J Mol Biol 305(3):581–592
31. Rousseau R et al (2004) Temperature-dependent conformational transitions and hydrogen-bond dynamics of the elastin-like octapeptide GVG(VPGVG): a molecular-dynamics study. Biophys J 86(3):1393–1407
32. Arkin H, Bilsel M (2010) Conformational transition in elastin polypeptide with different residue length. AIP Conf Proc 1203:1211–1216
33. Arkin H, Bilsel M (2009) Conformational transition in elastin polypeptide with different residue length. In: 7th international conference of the Balkan physical union, vols 1 and 2. 1203:1211–1216

34. Fratzl P (ed) (2008) Collagen: structure and mechanics. Springer, New York
35. Buehler MJ, Yung YC (2009) Deformation and failure of protein materials in physiologically extreme conditions and disease. Nat Mater 8(3):175–188
36. Rainey J, Wen C, Goh M (2002) Hierarchical assembly and the onset of banding in fibrous long spacing collagen revealed by atomic force microscopy. Matrix Biol 21(8):647–660
37. Eppell SJ et al (2006) Nano measurements with micro-devices: mechanical properties of hydrated collagen fibrils. J R Soc Interface 3(6):117–121
38. Rainey J, Goh M (2002) A statistically derived parameterization for the collagen triple-helix. Protein Sci 11(11):2748–2754
39. Huang CC et al (1998) The object technology framework: an object-oriented interface to molecular data and its application to collagen. Pac Symp Biocomput 349–361
40. Rainey J, Goh M (2004) An interactive triple-helical collagen builder. Bioinformatics 20(15):2458–2459
41. Persikov AV, Ramshaw JAM, Brodsky B (2005) Prediction of collagen stability from amino acid sequence. J Biol Chem 280(19):19343–19349
42. Boote C et al (2008) Collagen organization in the chicken cornea and structural alterations in the retinopathy, globe enlarged (rge) phenotype – an X-ray diffraction study. J Struct Biol 161(1):1–8
43. Orgel JPRO et al (2006) Microfibrillar structure of type I collagen in situ. Proc Natl Acad Sci 103(24):9001–9005
44. Sweeney SM et al (2008) Candidate cell and matrix interaction domains on the collagen fibril, the predominant protein of vertebrates. J Biol Chem 283(30):21187–21197
45. Brodsky B, Eikenberry EF, Cassidy K (1980) An unusual collagen periodicity in skin. Biochim Biophys Acta Protein Struct 621(1):162–166
46. Stinson RH, Sweeny PR (1980) Skin collagen has an unusual d-spacing. Biochim Biophys Acta Protein Struct 621(1):158–161
47. Gathercole LJ, Shah JS, Nave C (1987) Skin-tendon differences in collagen D-period are not geometric or stretch-related artefacts. Int J Biol Macromol 9(3):181–183
48. Sun YL, Luo ZP, An KN (2001) Stretching short biopolymers using optical tweezers. Biochem Biophys Res Commun 286(4):826–830
49. Sun YL et al (2004) Stretching type II collagen with optical tweezers. J Biomech 37(11):1665–1669
50. Buehler MJ, Wong SY (2007) Entropic elasticity controls nanomechanics of single tropocollagen molecules. Biophys J 93(1):37–43
51. Sun YL et al (2002) Direct quantification of the flexibility of type I collagen monomer. Biochem Biophys Res Commun 295(2):382–386
52. Chang S-W, Sandra J, Shefelbine SJ, Buehler MJ (2012) Structural and mechanical differences between collagen homo- and heterotrimers: relevance for the molecular origin of brittle bone disease. Biophys J 102(3):640–648
53. Chang S-W et al (2012) Molecular mechanism of force induced stabilization of collagen against enzymatic breakdown. Biomaterials 33(15):3852–3859
54. Bodian DL et al (2011) Molecular dynamics simulations of the full triple helical region of collagen type I provide an atomic scale view of the protein's regional heterogeneity. Pac Symp Biocomput 193–204
55. Adhikari AS, Chai J, Dunn AR (2011) Mechanical load induces a 100-fold increase in the rate of collagen proteolysis by MMP-1. J Am Chem Soc 133(6):1686–1689
56. Adhikari AS, Glassey E, Dunn AR (2012) Conformational dynamics accompanying the proteolytic degradation of trimeric collagen I by collagenases. J Am Chem Soc 134(32):13259–13265
57. Camp RJ et al (2011) Molecular mechanochemistry: low force switch slows enzymatic cleavage of human type I collagen monomer. J Am Chem Soc 133(11):4073–4078
58. Hofmann H et al (1984) Localization of flexible sites in thread-like molecules from electron-micrographs – comparison of interstitial, basement-membrane and intima collagens. J Mol Biol 172(3):325–343

59. Sasaki N, Odajima S (1996) Stress–strain curve and Young's modulus of a collagen molecule as determined by the X-ray diffraction technique. J Biomech 29(5):655–658
60. Cusack S, Miller A (1979) Determination of the elastic-constants of collagen by brillouin light-scattering. J Mol Biol 135(1):39–51
61. Harley R et al (1977) Phonons and elastic-moduli of collagen and muscle. Nature 267(5608):285–287
62. Gautieri A et al (2011) Hierarchical structure and nanomechanics of collagen microfibrils from the atomistic scale up. Nano Lett 11(2):757–766
63. Beck K et al (2000) Destabilization of osteogenesis imperfecta collagen-like model peptides correlates with the identity of the residue replacing glycine. Proc Natl Acad Sci 97(8):4273–4278
64. Gautieri A et al (2012) Osteogenesis imperfecta mutations lead to local tropocollagen unfolding and disruption of H-bond network. RSC Advances 2(9):3890–3896
65. Gautieri A et al (2009) Molecular and mesoscale mechanisms of osteogenesis imperfecta disease in collagen fibrils. Biophys J 97(3):857–865
66. Camacho NP et al (1999) The material basis for reduced mechanical properties in oim mice bones. J Bone Miner Res 14(2):264–272
67. Miles CA et al (2002) The role of alpha2 chain in the stabilization of the collagen type I heterotrimer: a study of the type I homotrimer in oim mouse tissues. J Mol Biol 321:797–805
68. Waterhouse A et al (2011) Elastin as a nonthrombogenic biomaterial. Tissue Engr Part B-Rev 17(2):93–99
69. Glowacki J, Mizuno S (2008) Collagen scaffolds for tissue engineering. Biopolymers 89(5):338–344
70. Wise SG et al (2005) Specificity in the coacervation of tropoelastin: solvent exposed lysines. J Struct Biol 149(3):273–281
71. Tarakanova A, Weiss A, Buehler MJ (2013) Elastic network model of tropoelastin implicated bridge region in assembly and cell-binding (In Preparation)
72. Orgel JPRO et al (2006) Microfibrillar structure of type I collagen in situ. Proc Natl Acad Sci USA 103(24):9001–9005